World Academy of Science, Engineering and Technology
International Journal of Chemical and Molecular Engineering
Vol:5, No:4, 2011

Preparation of Nanosized Iron Oxide and their Photocatalytic Properties for Congo Red

Akram Hosseinian, Hourieh Rezaei, Ali Reza Mahjoub

***Abstract*—**Nanostructured Iron Oxide with different morphologies of rod-like and granular have been suc-cessfully prepared via a solid-state reaction in the presence of NaCl, NaBr, NaI and NaN_3, respectively. The added salts not only prevent a drastic increase in the size of the products but also provide suitable conditions for the oriented growth of primary nanoparticles. The formation mechanisms of these materials by solid-state reaction at ambient temperature are proposed. The photocatalytic experiments for congo red (CR) have demonstrated that the mixture of α-Fe_2O_3 and Fe_3O_4 nanostructures were more efficient than α-Fe_2O_3 nanostructures.

***Keywords*—**Nano, Iron Oxide, Solid-State, Halide salts, Congo red

I. Introduction

THE synthesis of oxide nanoparticles attracts more and more attention because these nanoparticles exhibit electrical, optical and magnetic properties that are different from their bulk counterparts [1]. Iron oxides include α-Fe_2O_3, γ-Fe_2O_3 and Fe_3O_4. Among these Iron oxides, α-Fe_2O_3 has the corundum structure, while the other two have the cubic structure [2,3]. The study of Iron oxides has attracted intensive attention over the past decades due to the potential applications in catalysts [4-6], gas sensors [7], high density magnetic recording media [8], printing ink [9], ferrofluid [10], magnetic resonance imaging [11] and especially biomedical field [12,13], etc. Photocatalytic processes at semiconductor have received remarkable attention because of their potential application to the conversion of solar energy into chemical energy and pollution control [14].Various methods have been reported for the synthesis of Iron oxide nanostructures. These methods include reduction of iron salts in micelles [15,16], thermal reactions [17,18] using the electrochemical method [19], co-precipitation [20], microemulsion [21], hydrothermal synthesis [22] and sol gel method [23] etc. All these methods to Iron oxide nanostructures are in general complicated and expensive. There are many advantages in the solid-state reaction approach such as: (a) simple, cheaper and convenient; (b) involve less solvent and reduce contamination; (c) give high yields of products [24]. The photoassisted catalytic degradation of the dyes occurs by the active species created on the surface of metal-oxide semiconductor nanostructures in aqueous solution.

F. A. Author is with Department of Engineering Science, Engineering Faculty, University of Tehran, 11155-4563 Tehran, Iran. (e-mail: hoseinian@ut.ac.ir).
S. B. Author, is with Department of Chemistry, Tarbiat Modares University, 14115-175 Tehran, Iran (phone: +98-021-82883442; fax: +98-021-82883442; (e-mail: horizon.sea@gmail.com).
T. C. Author is with Department of Chemistry, Tarbiat Modares University, 14115-175 Tehran, Iran (phone: +98-021-82883442; fax: +98-021-82883442; (e-mail: mahjouba@modares.ac.ir).

Also the photogenerated electron–hole pair has a life span in the space charge region which facilitates its dynamic involvement in chemical reactions under the irradiation of proper energy [16]. In this paper, we synthesize Iron oxide nanostructures with different morphologies by solid-state reaction method. Our studies show that this method is not only a simple process but also gives as uniform and monodiesperse products as those by other lucrative methods. We have also investigated the effect of halogen and pseudo halogen salts on the morphology and explained in light of the proposed mechanisms. We found that the mixture of α-Fe_2O_3 and Fe_3O_4 nanostructures were more efficient than α-Fe_2O_3 nanostructures for CR photodegradation.

II. Experimental

A. *Preparation*

A mixture of $FeCl_2.4H_2O$ (1 mmol, 0.199 g), $FeCl_3$ (2 mmol, 0.324 g) and NaOH (8 mmol, 0.32 g) powders was ground for 15 min.Then, each of NaCl, NaBr, NaI and NaN_3 salts with a weight ratio of 1:2:6 was added to the system and ground for another 15 min at room temperature. The reaction began immediately during the mixing process (accompanying an emission of water vapor from the system). The powder was calcined at 500 ˚C for 1 hour in air and washed with distilled water for removing the halogen salt and dried in 60 ˚C.

B. *Characterization*

The morphology of Iron oxide powders was determined by using scanning electron microscopy (SEM) of a Holland Philips XL30 microscope. X-ray powder diffraction (XRD) patterns of the powders were recorded in ambient air with using a Holland Philips Xpert X-ray powder diffraction (Co Kα =1.78897 Å), at scanning 2˚ min^{-1} from 10˚ to 80˚ (2θ).

C. *Measurement of Photocatalytic Activity*

The evaluation of photocatalytic activity for the prepared samples decolorizing CR aqueous solution was performed at ambient temperature. The obtained Iron Oxide catalyst (0.01g) was placed into a beaker of 35 mL 10 mg/L CR aqueous solution. photocatalytic degradation of CR on the Iron Oxide nanoparticles was carried out under irradiation of sunlight, After the reaction began, the mixture was sampled at different times and separated by centrifuging. Then, absorption spectra were obtained through a wavelength scan on a UV-Vis spectrophotometer.

III. Results and Discussion

A. *Characterization of Iron Oxide*

The IR of the sample is shown in Fig.1a-d. The sample showed absorption in the regions 3430, 539 and 460 cm^{-1} . The general range of 3600–3100 cm^{-1} may be assigned to anti-Symmetrical and symmetrical O–H bonding stretching

vibrational modes for water of hydration. The bonding in the region of the bands at 460 and 539 cm^{-1} observed in sample can be attributed to metal oxygen stretching vibrational modes [25].

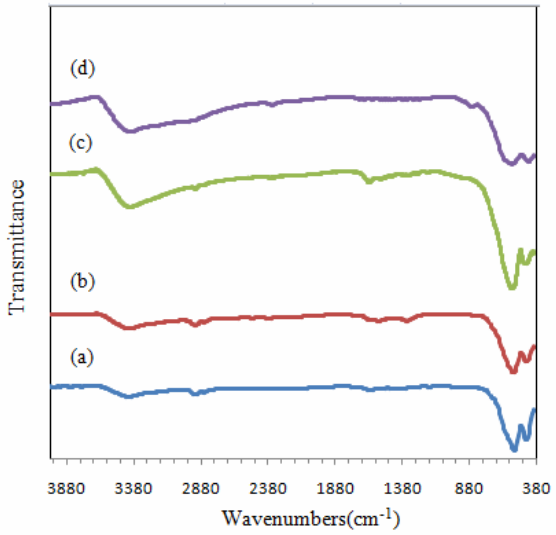

Fig. 1 The IR spectra of (a) NaCl500 (granular), (b) NaBr500 (granular), (c) NaI500 (granular), (d) $NaN_3$500 (rod-like)

The structure of Iron oxide powders was determined by XRD, as shown in Fig.2 a-d.The crystal grain sizes were calculated from the FWHM in XRD pattern using the Debye–Scherrer's equation and listed in Table1.Fig.2a and 2b indicates a pure rhombohedral crystalline phase of α-Fe_2O_3. The XRD patterns of NaBr 500 are shown in Fig.2c, a mixture of α-Fe_2O_3 and Fe_3O_4 phases were obtained. The ratio of (104) α-Fe_2O_3 peak to (220) Fe_3O_4 peak intensities, as a semiquantitative measure of α-Fe_2O_3/ Fe_3O_4 ratio, are included in Table1. The XRD patterns of NaN_3 500 are shown in Fig.2d, a mixture of γ-Fe_2O_3 and Fe_3O_4 phases were obtained.Scanning electron microscopy was employed to study the morphologies of the Iron oxide samples.Fig.3a–d shows that granular and rod-like morphologies of Iron oxide are formed, when halogen salts (NaCl, NaBr and NaI) and NaN_3 are used in the salt-assisted solid-state synthesis, respectively.

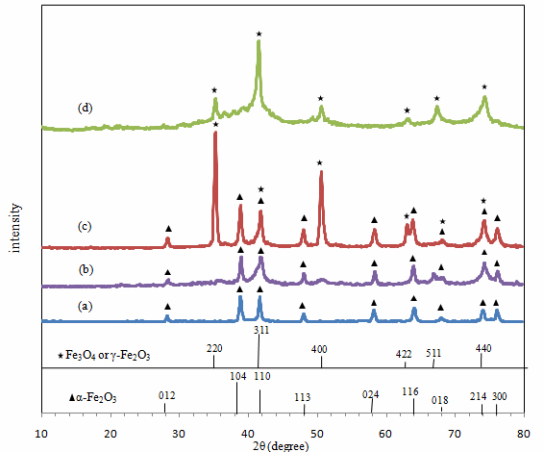

Fig. 2 XRD patterns of (a) NaCl500 (granular), (b) NaBr500 (granular), (c) NaI500 (granular), (d) $NaN_3$500 (rod-like)

TABLE I
THE SIZES, SEMIQUANTITATIVE MEASURE OF A-Fe_2O_3/ Fe_3O_4 RATIO AND PHYSICAL PROPERTIES OF THE AS PREPARED MATERIALS

Samples	Color	Morphology	Crystallite size (nm)	α-Fe_2O_3/ Fe_3O_4 (ratioof peaks intensity)
NaCl500	Reddish brown	nanoparticle	28.83	1:0
NaBr500	Dark brown	nanoparticle	30.32	1:3
NaI500	Reddish brown	nanoparticle	26.61	1:0
$NaN_3$500	Black-brown	nanorod	-	0:1

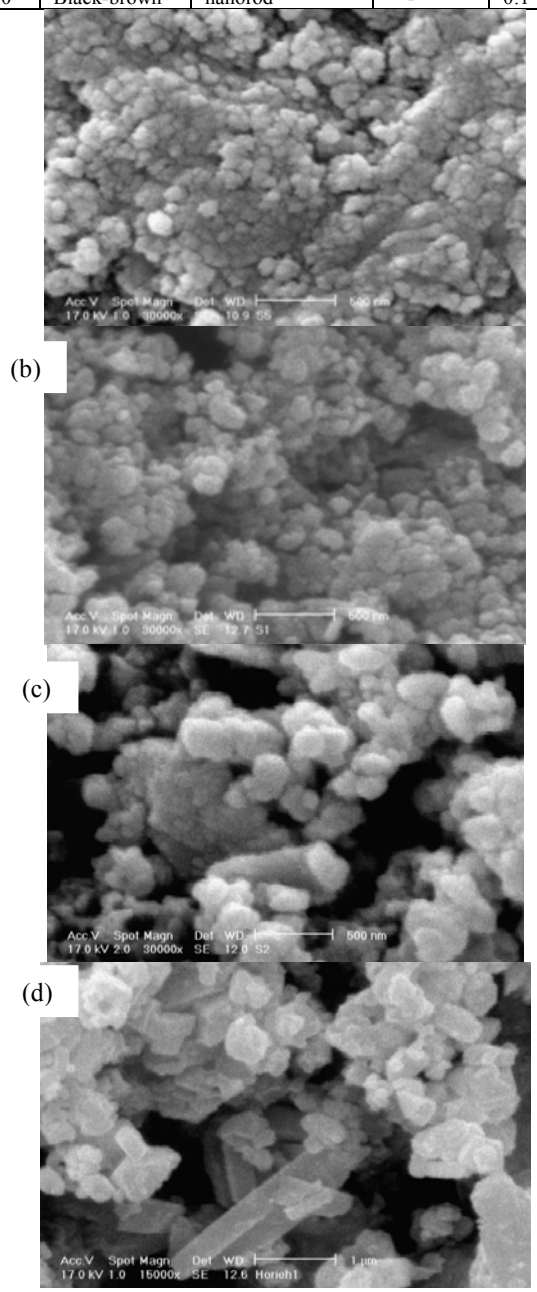

Fig. 3 The SEM images of (a) NaCl500 (granular), (b) NaBr500 (granular), (c) NaI500 (granular), (d) $NaN_3$500 (rod-like)

B. Mechanisms of Formation of Nanoparticles

The mechanisms of formation of nanoparticles via a solid-state reaction are discussed here.There are four steps in a typical proceeding of solid-state reaction: diffusion, reaction, nucleation and growth . $FeCl_2.4H_2O$ and $FeCl_3$ react with NaOH to produce Fe_2O_3 and Fe_3O_4 nanoparticles. $FeCl_2.4H_2O$ (s) + $FeCl_3$ (s) + NaOH (s) → Fe_2O_3 / Fe_3O_4 (nanoparticles) + NaCl + H_2O.

When Iron salts are mixed and ground with NaOH, they conjunct only at the border point, where several Iron salts atoms or molecules react with NaOH first. As the grinding continues, the further conjunction, reaction and diffusion are continuing in the system, more cores are obtained and the sizes of the cores are determined by the ratio of nucleation and growth of the products [26]. It is also thought that adding inorganic salts causes to reduce the overall reaction rate and broaden the distribution of product. NaCl, NaBr, NaI and NaN_3 as salt-assisted additives are expected to cause cage-like shells surrounding the cores and preventing their growth. Adjacent nanoparticles rotate to find the low-energy configuration represented by a coherent particle–particle interface [24]. As a result, the added salts help to form of suitable morphology with high yields.

C. Photo catalytic Properties for Congo Red

To evaluate the potential application in water treatment of the obtained a Iron Oxide nanoparticles, the photocatalysis capacities for the organic pollutant were investigated. Here, CR was chosen as the model organic pollutant. The initial concentration of the CR solution was set to be 10 mg/L. Fig.4a-d shows the Uv-vis absorption spectra of degradation the CR solution by obtained Iron Oxide nanoparticles with different times.The degradation of Congo Red dye was recorded as a function of time in the presence of visible light as shown in Fig.4a. The experimental data were found to fit approximately a pseudo-first-order kinetic model by the linear transforms $\ln(C_0/C) = f(t) = kt$ (k is rate constant), as shown in Fig. 4b.

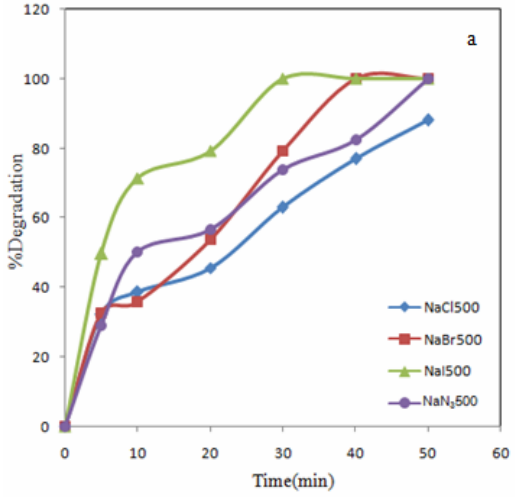

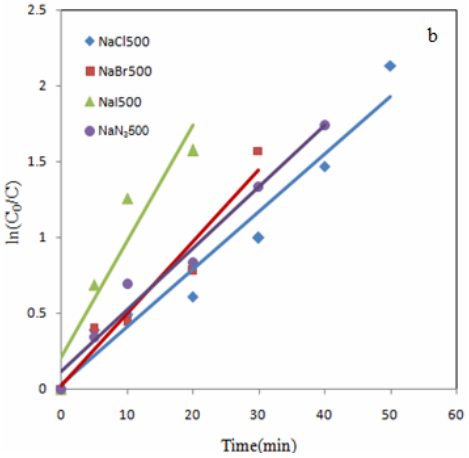

Fig. 4 (a) Photocatalytic degradation of congo red on Iron oxide nanoparticles under visible light irradiation; (b) Kinetics of different irradiation time

Maximum absorbance occur at about 560 nm for all samples. The highest percent of CR photodegradation is observed for NaI500 and the lowest percent of CR photodegradation is observed for NaCl500, as shown in Fig. 5. Comparison the photocatalysis performance between NaCl500 and NaI500 demonstrates the photocatalytic properties of Iron oxide semiconductors decreases, as their sizes increase, due to lower surface areas and comparison between NaCl500, NaBr500 and $NaN_3$500 demonstrates the mixture of α-Fe_2O_3 and Fe_3O_4 nanostructures are more efficient than α-Fe_2O_3 nanostructures because under the visible radiation, electrons in the valence band (CB) of α-Fe_2O_3 were excited to its conduction band (CB), with same amount of holes left in VB. Driven by the decreased potential energy (band gap of α-Fe_2O_3 is ~2.20 ev and band gap of Fe_3O_4 is ~0.10 ev), the photogenerated electrons in CB of α-Fe_2O_3 tended to transfer to that of Fe_3O_4, which reduced their recombination probability [17].

TABLE II
THE APPARENT RATE CONSTANTS OF THE CONGO RED DYE DECOMPOSITION REACTION

Name	time	Degradation	$K_{app}(min^{-1})$	R^2
NaCl500	50 min	88.16%	0.038	0.953
NaBr500(first)	40 min	100%	0.047	0.945
NaBr500(second)	50 min	100%	0.037	0.988
NaBr500(third)	50min	88.53%	0.037	0.911
NaI500	30 min	100%	0.076	0.888
$NaN_3$500	50 min	100%	0.040	0.974

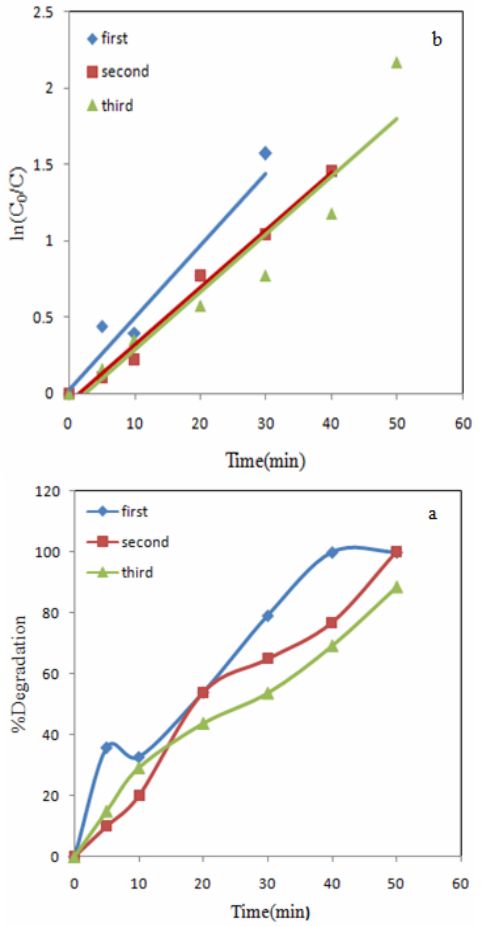

Fig. 5 Degradation of CR on NaBr500 for the first, second and third cycles; (b) Kinetics of different irradiation time

Furthermore, the used of Iron Oxide nanostructure can be recycled by a simple washing with distilled water. Fig.5. shows the CR photodegradation of NaBr500 for two and three cycles.

The obtained values of the apparent rate constants (K_{app}) of the reactions and the percent of degradation of congo red on Iron oxide nanoparticles are summarized in Table2. The results revealed that photodegradation of Congo red dyeobeyed the rules of a pseudo first-order kinetic reaction.

IV. Conclusion

We report the preparation of granular and rod-like morphologies of Iron oxide by solid-state reactions in the presence of NaCl, NaBr, NaI, and NaN_3 salts, respectively. The salts added are expected to cause cage-like shells surrounding the Iron oxides particles, preventing their growth of nanoparticles. The photocatalytic experiments showed that the mixture of α-Fe_2O_3 and Fe_3O_4 nanostructures are more efficient than α-Fe_2O_3 nanostructures.

References

[1] H. Xu, X. Wang, L. Zhang, Powder Technology, 185 (2008) 176.
[2] J. Lu, Sh. Yang, K. Ming, Ch. Su, Ch. Yeh, Y. Wu, D. Shieh, Nanotechnology, 17 (2006) 5812.
[3] X. Batlle, A. Labarta, J. Phys. D: Appl. Phys., 35 (2002) 15.
[4] D. Huang, D. Cao, Y. Li, H. Jiao, J. Phys. Chem. B, 110 (2006) 13920.
[5] O. Shekhah, W. Ranke, A. Schule, G. Kolios, R. Schlogl, Angew. Chem. Int. Ed. Engl., 42 (2003) 5760.
[6] P. Li, D. Miser, S. Rabiei, R. Yadav, M.R. Hajaligol, Appl. Catal. B, Environ. 43 (2003) 151.
[7] H. Zeng, J. Li, J.P. Liu, Z.L. Wang, S.H. Sun, Nature, 420 (2002) 395.
[8] C.T. Black, C.B. Murray, R.L. Sandstrom, S. Sun, Science, 290 (2000) 1131.
[9] T. Atarashi, T. Imai, J. Shimoiizaka, J. Magn. Magn. Mater., 85 (1990) 3.
[10] K. Raj, B. Moskowitz, R. Casciari, J. Magn. Magn. Mater., 149 (1995) 174.
[11] L.X. Tifenauer, A. Tschirky, G. Kuhne, R. Andres, Magn. Reson. Imaging, 14 (1996) 391.
[12] Z. Berkova, J. Kriz, P. Girman, K. Zacharovova, T. Koblas, E. Dovolilova, F. Saudek, Transplant Proc, 37 (2005) 3496.
[13] F. Mishima, S. Takeda, Y. Izumi, S. Nishijima, IEEE Trans. Appl. Supercond., 16 (2006) 1539.
[14] J. Zhong,Ch. Cao. Sensors and Actuators B, 145 (2010) 651.
[15] R.M. Cornell, U. Schwertmann,The Iron Oxides, VCH, NewYork, 1996.
[16] J.P. Wilcoxon, P.P. Provencio, J. Phys. Chem. B, 103 (1999) 9809.
[17] C.T. Seip, C. Connor, Nanostruct. Mater., 12 (1999) 183.
[18] T.W. Smith, D. Wychlck, J. Phys. Chem. B, 103 (1999) 9809.
[19] J. Van Wonterghem, S. Morup, Phys. Rev. Lett., 55(1985) 410.
[20] W.Q. Jiang, H.C. Yang, S.Y. Yang, H.E. Horng, J.C. Hung, Y.C. Chen, C.Y. Hong, J. Magn. Magn. Mater., 283 (2004) 210.
[21] D.E. Zhang, Z.W. Tong, S.Z. Li, X.B. Zhang, A.L. Ying, Mater. Lett., 62 (2008) 4053.
[22] M.Z. Wu, Y. Xing, Y.S. Jia, H.L. Niu, N.P. Qi, J. Ye, Q.W. Chen, Chem.Phys. Lett., 401 (2005) 374.
[23] J. Xu, H.B. Yang, W.Y. Fu, K. Du, Y.M. Sui, J.J. Chen, Y. Zeng, M.H. Li, G.G. Zou, J.Magn. Magn. Mater., 309 (2007) 307.
[24] A.A. Firooz, A.R. Mahjoub, A.A. Khodadadi, Materials Chemistry and Physics, 115 (2009) 196.
[25] S.K. Apte, S.D. Naik, R.S. Sonawane, B.B. Kalew, J. Am. Ceram. Soc., 90 (2007) 412.
[26] F. Li, X. Yu, H. Pan, M. Wang, X. Xin, Solid State Sciences, 2 (2000) 767.